

# *In Vivo* Validation of Numerical Prediction of Blood Flow in Arterial Bypass Grafts

JOY P. KU,<sup>1</sup> MARY T. DRANEY,<sup>2</sup> FRANK R. ARKO,<sup>3</sup> W. ANTHONY LEE,<sup>3</sup> FRANDICS P. CHAN,<sup>4</sup>  
NORBERT J. PELC,<sup>4</sup> CHRISTOPHER K. ZARINS,<sup>3</sup> and CHARLES A. TAYLOR<sup>2,3</sup>

<sup>1</sup>Department of Electrical Engineering, Stanford University, Stanford, CA; <sup>2</sup>Department of Mechanical Engineering, Stanford University, Stanford, CA; <sup>3</sup>Division of Vascular Surgery, Department of Surgery, Stanford University, Stanford, CA; and <sup>4</sup>Department of Radiology, Stanford University, Stanford, CA

(Received 13 December 2001; accepted 30 April 2002)

**Abstract**—In planning operations for patients with cardiovascular disease, vascular surgeons rely on their training, past experiences with patients with similar conditions, and diagnostic imaging data. However, variability in patient anatomy and physiology makes it difficult to quantitatively predict the surgical outcome for a specific patient *a priori*. We have developed a simulation-based medical planning system that utilizes three-dimensional finite-element analysis methods and patient-specific anatomic and physiologic information to predict changes in blood flow resulting from surgical bypass procedures. In order to apply these computational methods, they must be validated against direct experimental measurements. In this study, we compared *in vivo* flow measurements obtained using magnetic resonance imaging techniques to calculated flow values predicted using our analysis methods in thoraco-thoraco aortic bypass procedures in eight pigs. Predicted average flow rates and flow rate waveforms were compared for two locations. The predicted and measured waveforms had similar shapes and amplitudes, while flow distribution predictions were within 10.6% of the experimental data. The average absolute difference in the bypass-to-inlet blood flow ratio was  $5.4 \pm 2.8\%$ . For the aorta-to-inlet blood flow ratio, the average absolute difference was  $6.0 \pm 3.3\%$ . © 2002 Biomedical Engineering Society. [DOI: 10.1114/1.1496086]

**Keywords**—Computational fluid dynamics, Magnetic resonance imaging, Surgical planning.

## INTRODUCTION

Atherosclerotic lesions that result in critical arterial stenoses are often treated with surgical bypass grafts. These operations are planned using diagnostic data and empirical data derived from a physician's training and prior experience with other patients. However, this empirical approach to surgical planning does not account

for specific anatomic and physiologic variability among subjects. Furthermore, the preoperative diagnostic imaging data are of limited value in quantitatively predicting the efficacy of a treatment plan for an individual patient. We have recently proposed a new paradigm for surgical planning, in which numerical simulation methods are applied to patient-specific anatomic and physiologic models to predict changes in blood flow for alternative surgical procedures.<sup>32</sup> Numerical simulation methods have been used extensively to study the relationship between the fluid mechanics of blood and the development of arterial disease<sup>6,12,13,25,31,33</sup> and to test hypotheses regarding the effects of different parameters of bypass graft surgery on hemodynamic factors.<sup>8,10,11,14,15,27,29</sup> Recently, Taylor *et al.* described a comprehensive system for simulation-based medical planning to enable the preoperative assessment of alternate treatment plans.<sup>32</sup> In this system, numerical methods were utilized to predict blood flow and pressures in postoperative models given patient-specific anatomic and physiologic data. The advantage of using numerical simulations for these investigations is its ease of use over physical testing. Numerical simulations can provide a more complete description of hemodynamic conditions than experimental fluid mechanical methods. Furthermore, numerical models can be readily modified to assess the effects of a given parameter, such as the bypass graft angle or the graft-to-host-artery diameter.

Prior to applying these methods, validation studies are needed to verify the accuracy of the results predicted using numerical simulation methods. Previous *in vitro* experiments have demonstrated favorable agreement between the velocity profiles calculated using numerical simulations and those measured using phase contrast magnetic resonance imaging (PC-MRI).<sup>3,21,28</sup> Similarly, favorable agreement was obtained when comparing numerical simulation results of velocity profiles to laser Doppler anemometry measurements in an end-to-side

Address correspondence to Charles A. Taylor, Assistant Professor of Surgery and Mechanical Engineering, Durand 213, Stanford University, Stanford, CA 94305-3030. Electronic mail: taylorca@stanford.edu

Present address for W. Anthony Lee: Section of Vascular Surgery, Department of Surgery, University of Florida College of Medicine, Gainesville, FL 32610.

anastomosis model.<sup>16,30</sup> The agreement obtained between numerical and *in vitro* experimental results is encouraging, but validation studies are needed to fully assess the usefulness of these computational methods *in vivo*. *In vitro* experiments fail to incorporate all the complexities observed *in vivo*. For example, the models are rigid and do not replicate the compliant nature of blood vessels, and the blood-mimicking materials used in the experiments are Newtonian fluids, rather than suspensions of cells in plasma like blood. Furthermore, these *in vitro* studies have been performed using idealized geometric and physiologic parameters, so the results do not accurately describe the blood flow for a specific patient.

Thus far, few *in vivo* validations have been performed because noninvasive methods for obtaining both *in vivo* measurements of blood flow and high-resolution three-dimensional anatomic information have not been available. While computed tomography provides the three-dimensional anatomic information, it cannot measure blood flow. Ultrasound can be used to acquire three-dimensional anatomic and physiologic data, but this is limited to certain anatomic regions and through-plane velocity profiles cannot be obtained. However, advancements in magnetic resonance imaging (MRI), such as velocity mapping<sup>24</sup> and ultrafast magnetic resonance angiography (MRA),<sup>1</sup> have made it possible to obtain blood flow measurements and three-dimensional anatomic information with a single imaging modality, making it ideal for *in vivo* validations of numerical analysis methods for blood flow.

Long *et al.* have utilized MRI to examine the accuracy of simulation methods in the aortoiliac bifurcation region<sup>18</sup> and in the carotid artery<sup>17</sup> for one subject. These investigations demonstrated good agreement between the numerical results and the MRI velocity measurements. In both of these studies, inlet and outlet velocity boundary conditions were specified using MRI data, and the predicted velocity was compared with MRI data on a plane midway between the inlet and outlet. While this approach is reasonable for investigations where the flow distribution can be fully specified, it is not applicable to surgery planning where the flow distribution is not known *a priori*.

In this paper, we present the results of a series of porcine studies designed to test the accuracy of the simulation-based medical planning system described above for an arterial bypass graft in the thoracic aorta. In each of the eight pigs studied, an aortic coarctation was created, and a graft was anastomosed to the thoracic aorta proximally and distally to bypass the coarctation (Fig. 1). This model resembles surgical bypasses of severe stenoses in patients using proximal and distal end-to-side anastomoses. Numerical simulations based on MRI-acquired anatomic and inlet flow information for each animal were performed. The numerically predicted

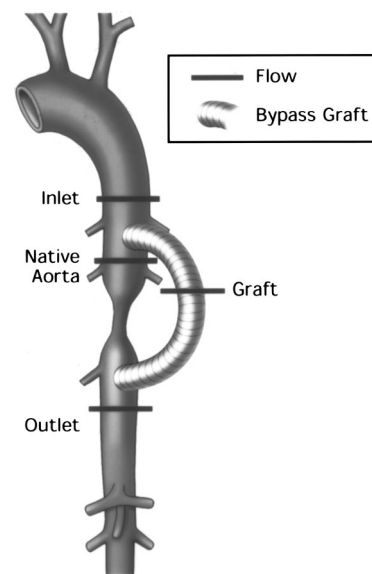


**FIGURE 1.** Diagram of the experimental protocol. A thoraco-thoraco aortic bypass procedure was performed to bypass an 80%–95% constriction of the descending thoracic aorta in the pig. Flow measurements were acquired using phase contrast magnetic resonance imaging at the four locations indicated. The inlet flow measurements were used as a boundary condition for the numerical simulations, while the flow rates at the aorta and at the graft were used for validation of the numerical simulations.

flow rates in the native aorta and in the bypass graft were found to be in good agreement with the corresponding MRI measurements. These favorable results provide the first *in vivo* validation of numerical methods applied to predict blood flow changes in arterial bypass graft procedures.

## MATERIALS AND METHODS

Eight Yorkshire cross pigs (36.5–48 kg) were used in this investigation. All animal procedures were approved by and performed in accordance with the policies set by the Institutional Animal Care and Use Committee.

### *Surgical Procedure*

Each animal was preanesthetized with telazol (5–7 mg/kg, IM) mixed with atropine (0.05 mg/kg) prior to endotracheal intubation. Animals were anesthetized with isoflurane (1%–4%) during the entire procedure, and ventilation was mechanically controlled. With the animal in a supine position, a longitudinal midline incision in the neck was used to isolate the internal jugular vein and common carotid artery. Arterial and venous access was obtained with 7F sheaths for monitoring purposes. A longitudinal incision in the right groin was used to isolate the common femoral artery that was accessed with a 7F sheath. After administration of pancuronium bromide

(0.11 mg/kg), a left anterolateral thoracotomy was performed and the descending thoracic aorta from the azygos vein to the diaphragmatic hiatus was exposed. A 150–300 IU/kg intravenous bolus of heparin sulfate was given to achieve an activated clotting time (ACT) greater than 250 s. The ACT was monitored every 30 min, and additional heparin was given as needed to maintain the ACT greater than 250 s. A side-biting vascular clamp was used to partially occlude the proximal thoracic aorta. An end-to-side anastomosis between the aorta and a 10 mm polyester fabric (Dacron) vascular graft was performed with a fine-running monofilament suture. The distal end of the graft was anastomosed to the distal descending thoracic aorta in a similar fashion. A polyester (Dacron) umbilical tape was tied around the thoracic aorta midway between the two anastomoses to create an 80%–95% stenosis. The thoracotomy incision was then sutured closed, and the animal was transported to the MRI suite while still monitored and ventilated under general anesthesia.

### *Magnetic Resonance Imaging*

Both vascular geometry and blood flow measurements were acquired using a 1.5 T MRI system (Signa, GE Medical Systems, Waukesha, WI). A wrap-around phased array coil was placed around the animal's abdomen for signal reception, and a respiratory sensor was wrapped around the animal's chest for monitoring respiration. The animal was placed in the magnet in the right decubitus position. Two-dimensional localizer images were obtained for spatial localizations of the subsequent scans.

Contrast-enhanced magnetic resonance angiography (CE-MRA) data were obtained using a rapid, three-dimensional, gradient-recalled echo sequence.<sup>1</sup> A 0.2 mmol/kg dose of Magnevist (Berlex Laboratories, Wayne, NJ), a gadolinium-based contrast agent, was injected into the animal via the 7F sheath in the internal jugular vein at a rate of 2.5–3 cc/s. A pretiming scan was performed to ensure that the acquisition occurred during maximum concentration of contrast in the thoracic aorta. The image acquisition was performed during suspended respiration with TR=3.76 to 4.9 ms depending on the field of view (FOV=24 to 32 cm), TE=0.90 to 1.07 ms, a maximum slice thickness of 2.6 mm zero filled to 1.3 mm slice spacing, an acquisition matrix size of 512 × 192, and a 25° flip angle. Between 80 and 100 slices were acquired in the axial direction.

Two methods were used to acquire the velocity information. For all pigs except pig C, a two-dimensional segmented  $k$ -space sequence<sup>5,9,34</sup> with TR=7 to 8 ms, TE=3.2 to 3.5 ms, FOV=24 cm, 5 mm slice thickness, 256 × 192 acquisition matrix, 4  $k$ -space lines per cardiac cycle, 30° flip angle, NEX=1, and ±350 cm/s maximum flow encoding was used to acquire the velocity compo-

nent along the vessel axis. Respiration was suspended during these scans. Pig C velocity data were acquired using a two-dimensional (2D) cine phase contrast sequence<sup>20,22</sup> to obtain three orthogonal components of velocity. The following parameters were used: through-plane velocity encoding between ±100 and ±350 cm/s, in-plane velocity encoding between ±50 and ±100 cm/s,<sup>37</sup> respiratory compensation, oversampling to prevent spatial aliasing (no phase wrap), TR=25 to 34 ms, TE = 4.0 to 4.3 ms, 24 cm FOV, 5 mm slice thickness, acquisition matrix of 256 × 256, NEX=1, and a 20° flip angle. For both methods, velocity acquisitions were synchronized using the signal from a photoplethysmograph attached to the animal. Twenty-four time points per cardiac cycle were reconstructed, and all flow calculations were based on this single, average cycle.

Velocity information was acquired at four locations: superior to the graft (inlet), between the proximal anastomosis and the aortic coarctation (native aorta), in the graft (graft), and distal to the graft (outlet) (Fig. 1). Volume flow rates for the four locations were computed by multiplying the average through-plane velocity by the cross-sectional area of the region of interest. Custom software was used to apply a baseline correction to the flow computations to account for eddy currents and to segment out the region of interest via thresholding of the magnitude images.<sup>23</sup>

### *Numerical Flow Simulations*

The process for generating the numerical flow solutions is depicted in Fig. 2. Currently, the entire process of acquiring imaging data, creating a geometric model, and running the flow simulations can be completed within 2 days, an acceptable time frame for the preoperative planning of many bypass graft procedures.

Using the CE-MRA data, geometric models of the thoracic aorta and the bypass graft were constructed with custom software. A spline fit through 5–10 manually selected points described paths through the vessels of interest. Two-dimensional slices were oriented perpendicular to these paths, and a level set method was applied to each of these slices to segment out the vessel lumen. The level set method that we have implemented performs segmentations based on image intensity gradients and user-specified curvature criteria.<sup>35,36</sup> This approach produces a segmentation that more closely matches the lumen shape than a circular fit while still maintaining the smoothness necessary for creating a solid model. Nonuniform rational B-spline (NURB) surfaces were lofted through the cross sections and bounded to create a solid model using the Parasolid (Unigraphics Solutions, St. Louis, MO) geometry kernel. This process was used to create solid models of the aorta and the bypass, which were then joined together to construct a

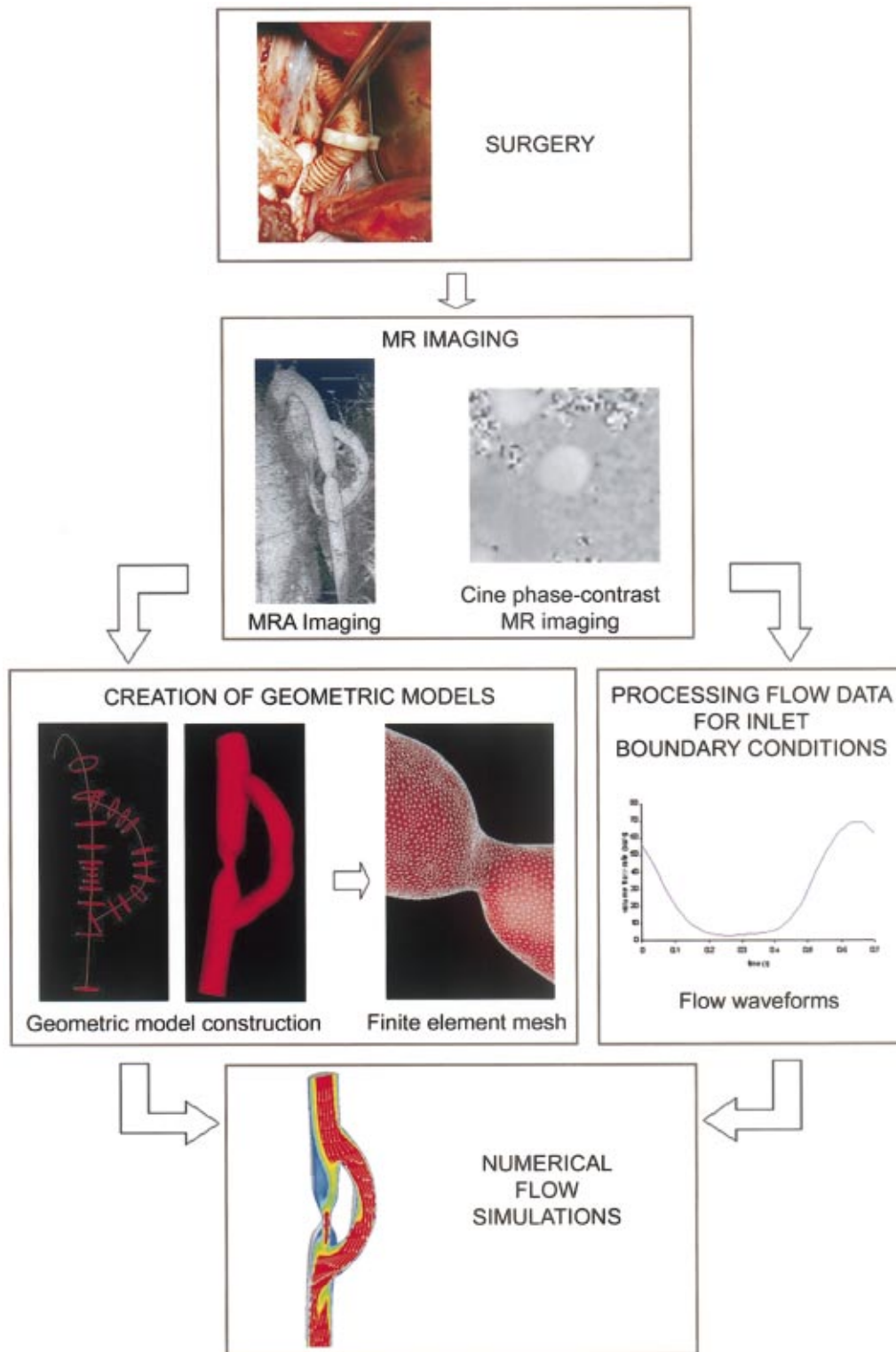


**FIGURE 2.** Process for generating numerical flow results. Magnetic resonance angiography (MRA) provided anatomic information from which a geometric model was constructed. The phase contrast image plane at the inlet was used to trim the geometric model. Automatic mesh generation software converted the solid geometric model to a finite-element mesh, which was used in the numerical simulation. The numerical simulation also required boundary conditions. The inlet flow velocity was acquired using phase contrast magnetic resonance imaging (PC-MRI) and integrated over the cross section to compute a flow rate, which in conjunction with pulsatile flow (Womersley) theory, was utilized as a boundary condition for these simulations.

final geometric solid model. The PC-MRI image plane at the inlet, approximately 1–2 cm proximal to the proximal anastomosis, was then used to trim the model.

Automatic mesh generation software<sup>26</sup> (MeshSim, Simmetrix, Inc., Clifton Park, NY) was used to discretize these models into finite-element meshes needed to compute the flow solutions. The inlet flow was described by an axisymmetric, fully developed, pulsatile flow (Womersley) velocity profile that was based upon the PC-MRI through-plane flow rate data at the inlet. While it is possible to directly utilize PC-MRI-acquired velocity data, these techniques were not available at the time this study was conducted. However, Favier and Taylor have shown that prescribing a Womersley velocity profile at the inlet of the bypass graft flow simulation for pig D produces the same downstream volumetric flow rates as setting the inlet velocities to experimentally measured values.<sup>7</sup> The area of the Womersley velocity profile was chosen to produce flow equivalent to experimentally measured flow. The area was computed using the center and equivalent-circle radius of the inlet mesh, where an equivalent-circle radius was defined as the radius of a circle with the same cross-sectional area as the inlet. These values were then mapped onto the inlet mesh. The velocities of the nodes on the inlet mesh which were further from the center than the equivalent-circle radius were set to zero. Those nodes on the boundary of the inlet mesh that were closer to the center than the equivalent-circle radius were also assigned to have zero velocity. Note that all boundary nodes were set to zero to enforce a no-slip boundary condition.

Since blood is incompressible, the walls were assumed to be rigid, the model had only one outlet, and velocity was prescribed at the inlet, the choice of exit pressure did not affect the velocity fields. We prescribed a zero exit pressure for all calculations. Velocities along the luminal surface of the aorta and the graft were prescribed to be zero, consistent with a no-slip condition. Blood was modeled as a Newtonian fluid with a constant density of 1.06 g/cm<sup>3</sup> and a constant viscosity of 0.04 dyn s/cm<sup>2</sup>, corresponding to the approximate asymptotic viscosity value of blood at high shear rates and normal hematocrit. Under these boundary conditions and assumptions, pulsatile flow was computed for five cardiac cycles using a previously validated stabilized finite-element method with linear tetrahedral elements that is second-order accurate in time to solve the incompressible Navier–Stokes equations.<sup>30</sup> These problems can be solved using 32 processors on a 128-processor Origin 3800 (Silicon Graphics, Inc., Mountain View, CA) in approximately 6 h. The fourth cycle of these solutions was used for the flow comparisons.

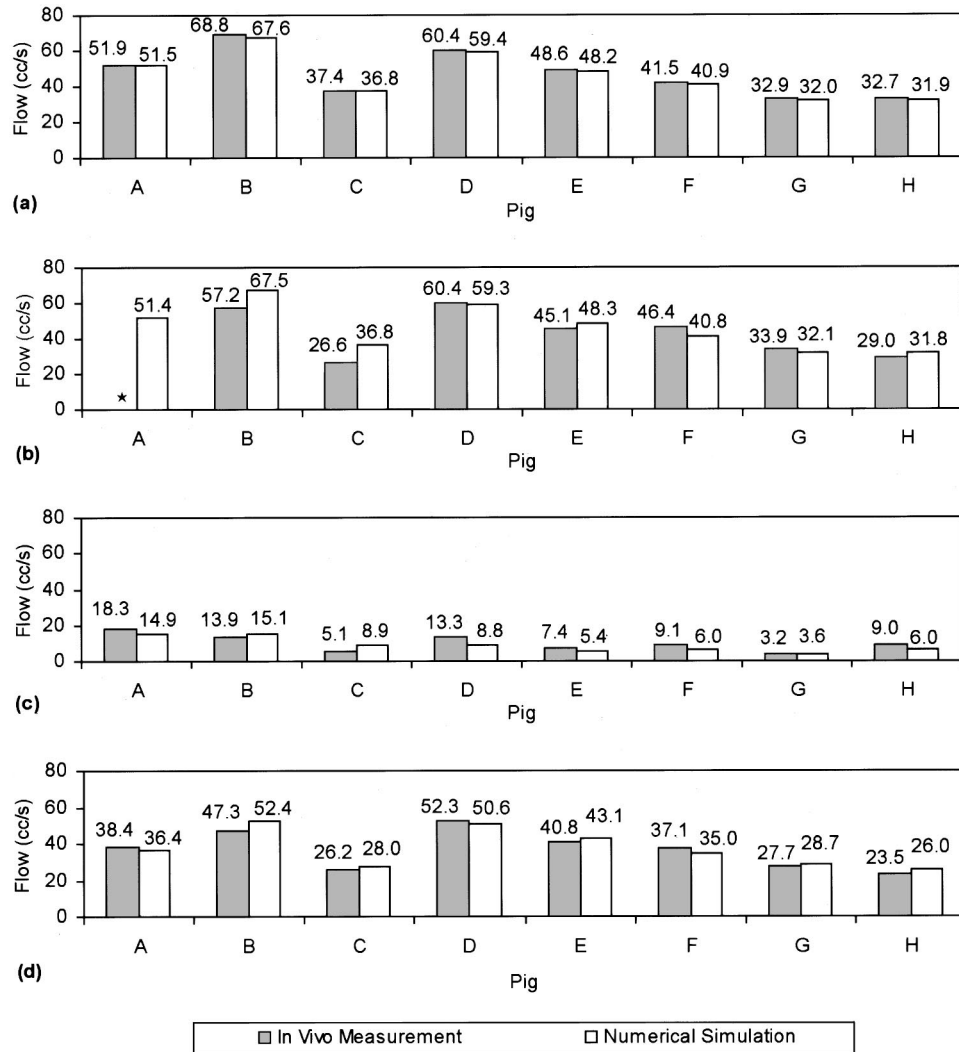
Convergence studies were conducted on pig D to determine the mesh size and the time increment to use in computing the flow solutions for these models. Compari-

sons were made of the flow solutions for meshes of 151,000 elements, 548,000 elements, and 1.24 million elements against results for a mesh with 1.85 million elements. The flow rates in the native aorta for the 151,000 element mesh showed an average absolute difference of 27%, while those of the 548,000 element mesh showed an average absolute difference of 13%. The average absolute difference was 5% for the 1.24 million element mesh. In the bypass, the flow rates were much higher, so the differences in flow due to mesh size were less significant. For the bypass flow rates, the average absolute difference was 7% in the 151,000 element mesh, 3% in the 548,000 element mesh, and 1% in the 1.24 million element mesh. In order to obtain an accurate result in a reasonable amount of time, the experiments were run with meshes of approximately 550,000 elements. The actual mesh sizes varied from 546,000 to 764,000 linear tetrahedral elements. The number of time steps per cardiac cycle was also varied for the flow solution of the 548,000 element mesh for pig D. The average absolute difference in flow rates for calculations performed for 240 vs 480 time steps per cardiac cycle was 2%, or  $0.15 \pm 0.12$  cc/s, in the native aorta and 0.4%, or  $0.16 \pm 0.13$  cc/s, in the bypass graft. Therefore, to reduce computation time, 240 time steps were used per cardiac cycle.

Additional models were created to examine the sensitivity of the simulated flow results to variations in the degree of stenosis. Since the cross-sectional area of the stenosis has the largest effect on the pressure drop, the lumen boundary acquired using the level set method for this region was scaled up and down for one pig (pig E) and changes in flow distribution were quantified. An equivalent-circle radius was defined as the radius of a circle with the same cross-sectional area as the segmented contour. The scale factor was determined by increasing and decreasing the equivalent-circle radius up to an amount equal to the pixel resolution of the MRA data acquired for that pig. The mesh and flow solutions for these modified models were produced using the same methods and under the same conditions as for the original model.

### Data Analysis

To verify the accuracy of our simulation methods, we used custom visualization software to calculate the blood flow rates from the computed velocity fields in the native aorta and in the bypass graft. These quantities were measured *in vivo* and compared with the computational results.



\*In vivo data not available

FIGURE 3. Comparison of predicted mean flow rates to measured mean flow rates through the (a) inlet, (b) outlet, (c) native aorta, and (d) bypass graft.

## RESULTS

The computational flow results were compared to the MRI measurements for all eight animals (Fig. 3). Volume blood flow through the thoraco–thoraco bypass graft was significantly greater than through the constricted thoracic aorta. This is consistent with theoretical predictions and was demonstrated by both MRI flow measurements and computational results. The MRI data showed that, on average, 3.2–18.3 cc/s of blood flowed through the native aorta, depending on the tightness of the surgically created stenosis. This was only 10%–35% of the blood that entered the descending thoracic aorta. The numerical solutions predicted similar results, differing from the MRI-measured aorta-to-inlet blood flow ratios by –10.6%–8.9%. The mean absolute difference in flow

ratios was  $6.0 \pm 3.3\%$  [Fig. 4(a)]. Good agreement between the MRI measurements and the numerical solutions was also observed for the blood flow through the bypass grafts, with the difference in the bypass-to-inlet blood flow ratios ranging from –9.7% to 3.6%. The mean absolute difference was  $5.4 \pm 2.8\%$  [Fig. 4(b)]. The difference in flow rates between *in vivo* measurements and simulation results ranged from –3.8 to 4.6 cc/s in the native aorta and from –5.1 to 2.0 cc/s in the bypass graft. The average absolute difference was  $2.7 \pm 1.4$  cc/s in the native aorta. In the bypass, the average absolute difference was  $2.3 \pm 1.2$  cc/s.

The MRI-measured and numerically computed flow rate waveforms appeared to have similar shapes and amplitudes (Fig. 5). Qualitatively, minor differences ex-

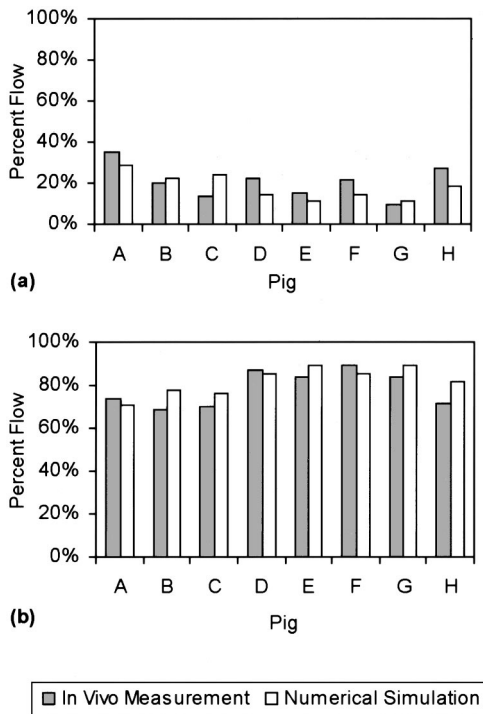


FIGURE 4. Comparison of predicted and measured (a) aorta-to-inlet flow ratio, and (b) bypass-to-inlet flow ratio.

isted between the MRI measurements and the numerical solutions. For instance, the MRI measurements showed a small amount of reverse flow in the aorta for four of the animals and in the bypass for one of the animals. However, this phenomenon was not observed in the corresponding numerical measurements. There was also a small time delay between the MRI-derived flow waveforms and the numerically computed flow waveforms in the native aorta and the bypass for pigs A, B, E, and F.

Figure 6 shows the flow distributions for pig E for different stenosis contours. As predicted theoretically, a tighter stenosis, which corresponds to a smaller equivalent-circle radius, caused more flow to be diverted through the bypass graft and less flow to go through the native aorta. The unaltered stenosis contour, as generated by the model construction process, had an equivalent circle radius of 1.38 mm. For an increase in equivalent-circle radius from 1.38 to 1.65 mm, 5% more blood flowed through the native aorta and 5% less blood flowed through the bypass graft. On the other hand, a decrease in equivalent-circle radius from 1.38 to 1.11 mm resulted in a 5% increase in blood flow in the bypass graft and a corresponding decrease in blood flow in the native aorta.

Heart rates for the animals were recorded every 10–20 min. The average heart rates for the animals ranged from 80 to 123 bpm during the imaging portion of the experiment. During this time, the animals' heart

rates varied, with the minimum variation in heart rate being 3 bpm and the maximum variation in heart rate being 29 bpm.

## DISCUSSION

Based on the eight animals studied, there is excellent agreement in flow rates and flow waveforms between the MRI measurements and the numerical simulation results. The maximum absolute difference in branch-to-inlet blood flow ratio was 10.6%. The average absolute difference in the aorta-to-inlet blood flow ratio was only 6.0%, while that of the bypass-to-inlet blood flow ratio was only 5.4%. Furthermore, the flow waveforms generated from the numerical simulations and from the experimental data appeared similar in shape and amplitude, suggesting that in addition to being able to accurately predict the time-averaged flow rates, the numerical methods could also reasonably predict flow rates for a given time point in the cardiac cycle.

The small differences that were observed between the simulation results and the MRI measurements can be attributed to both physiological conditions and technological limitations. The accuracy of the geometric model that is constructed has a significant impact on the resulting computational flow values. As the sensitivity study performed on pig E showed, imprecise modeling of the aortic constriction could lead to variation in the flow distribution. If the constriction was modeled to be tighter than it actually was, then the predicted flow rate in the bypass graft would be higher than the *in vivo* measurement, while the flow rate in the native aorta would be lower. This could explain the results observed in pig E. Increasing the equivalent-circle radius of the contour used to model the stenosis by 0.27 mm, half the pixel resolution of the MRA data set, caused 5% more blood flow in the native aorta and 5% less blood flow in the bypass graft, resulting in better agreement with the *in vivo* measurements. Other assumptions made in modeling the blood and blood vessels, such as the aforementioned Newtonian approximation of blood viscosity and a rigid wall assumption, could also cause discrepancies between the numerical results and the MRI measurements. Improvements to our modeling capabilities would allow for more realistic simulations that could test the effects of the simplifying assumptions that were used and potentially improve the agreement between the simulation and the *in vivo* flow results.

Changes in animal physiology and limitations of the MRI techniques could also lead to inconsistencies in the experimental measurements and account for some of the differences between the *in vivo* data and the numerical simulation results. Use of an inaccurate baseline correction during postprocessing of the *in vivo* measurements could lead to offsets in the velocity measurements and

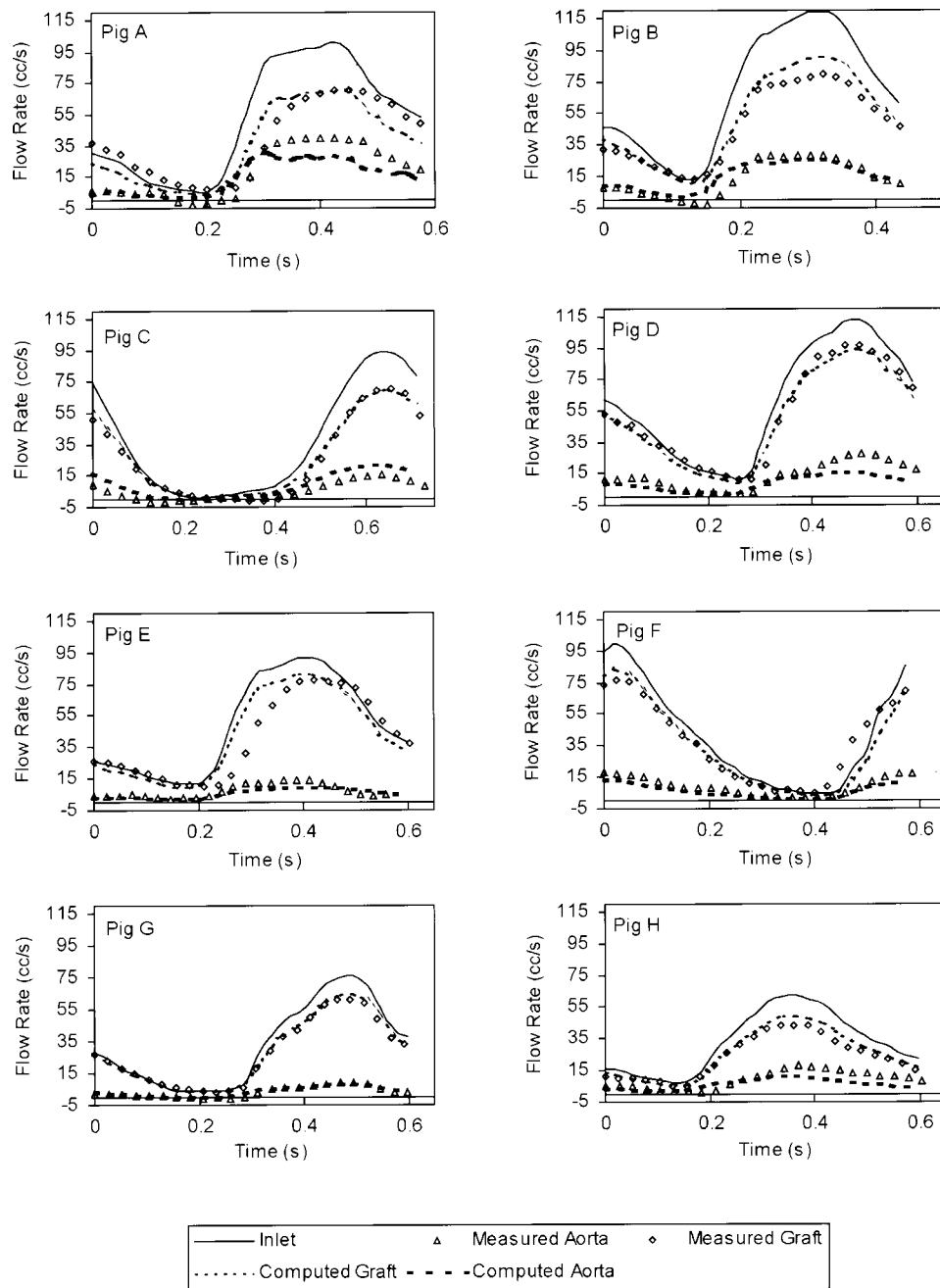


**FIGURE 5.** Comparison of predicted flow rates to measured flow rates over one cardiac cycle for eight pigs.

account for differences between the MRI-measured and the numerically computed flow waveforms. This could explain the differences observed in the native aorta flow waveforms for pigs C and F, in which the measured and computed waveforms appear to be offset from one another. We also observed that the measured flow rates did not strictly “conserve” flow. For the *in vivo* data, the sum of the mean flows in the bypass graft and through the native aorta differed from the inlet flow by as much as 22% of the inlet flow, while the difference between

the MR-measured inlet and outlet flows was as much as 28.9% of the inlet flow. The lack of conservation of flow in the MR data can produce results in which the numerically predicted aorta and bypass flows are both less than the measured flows, as in pig A. Possible explanations for the discrepancies in the MR measurements include inaccuracies in the imaging method<sup>4,19</sup> and the omission of outflow through small intercostal arteries due to experimental constraints. An alternative explanation is that the animal’s physiology changed between image acquisi-

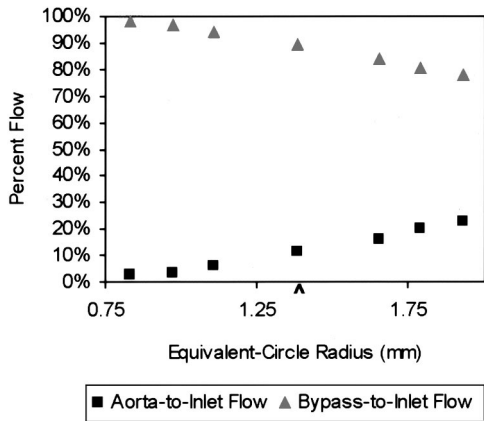


**FIGURE 6.** Sensitivity of the flow solutions to the equivalent-circle radius of the stenosis contour for pig E. The caret indicates the equivalent-circle radius of the original stenosis contour. The original stenosis contour was scaled to increase or decrease its equivalent-circle radius by 0.5, 0.75, or 1 pixel. As predicted theoretically, a tighter stenosis, which corresponds to smaller values of the equivalent-circle radius, caused more flow to be diverted through the bypass graft and less flow to go through the native aorta.

tions at different locations. Monitoring of the animals showed that heart rate varied by as much as 28 bpm during the data acquisition. Since the PC-MRI images were not acquired at all four locations simultaneously, any change in the animal's heart rate or blood flow distribution would only affect measurements for a single location, potentially leading to an apparent violation of conservation of flow. More detailed recordings of the animal physiology during image acquisition could verify this claim. Also, *in vitro* experiments would eliminate the variability due to changing animal physiology and permit investigation of the accuracy and reproducibility of the PC-MRI measurements.

This validation study focused on the prediction of blood flow distribution, an important quantity in vascular surgery, where a primary goal is restoration of flow to regions of low blood flow. It is also of great interest to be able to predict flow patterns and shear stresses, which have been shown to play a role in the development of atherosclerosis and may be correlated with the long-term effectiveness of bypass graft procedures.<sup>2,38</sup> Quantification of blood flow rate and distribution is a necessary condition for accurate prediction of flow velocity patterns and shear stresses. Evaluation of these more detailed predictions should be pursued.

The importance of the 5%–6% average difference observed between the numerical results and the MRI measurements is currently unknown, since this flow rate information has not previously been available to physicians. It is unknown how accurate blood flow simulations need to be in order to be useful to physicians, but the results from the eight animals studied here show that

the numerical results and the MRI measurements for the flow rates are similar. This suggests that given only input flow information and a geometric model, computational methods can be used to predict flow rates and flow distributions for bypass graft procedures similar to the one performed in this study.

Quantitative data on blood flow rates and distribution can aid surgeons in deciding how to treat a patient, providing additional information to be considered when weighing the risks of various treatment plans against the anticipated outcomes. Surgeons could simulate and compare different treatments, such as an aorta–femoral bypass surgery versus a femoral–femoral bypass procedure. In addition, they could use these computational methods to modify parameters, such as the anastomosis angle, the size of the bypass graft, or the enlargement of a vessel by angioplasty, and preoperatively determine the effect of these changes on flow distribution. Volumetric flow rate at the inlet could also be altered to allow the surgeon to predict blood flow changes under different physiologic conditions, such as exercise and rest. This is the first *in vivo* validation of these simulation methods and as such, it is an important step towards this new paradigm in medicine, in which surgeons can ascertain the effects of different vascular surgery treatment plans for a specific patient prior to actually performing the operation.

## ACKNOWLEDGMENTS

The authors thank K. Wedding, C. Elkins, W. Baumgardner, and D. Howard for their assistance with the experiments; S. Spicer, T. Brosnan, K. Wang, and N. Wilson for providing software; and W. Ong, R. Spilker, and G. Chan for helping with data processing. This work was done during the tenure of a fellowship from the American Heart Association, Western States Affiliate. Support was also provided by a NIST–ATP grant, NIH grant P41RR09784, and the Lucas Foundation.

## REFERENCES

- Alley, M. T., R. Y. Shifrin, N. J. Pelc, and R. J. Herfkens. Ultrafast contrast-enhanced three-dimensional MR angiography: State of the art. *Radiographics* 18:273–285, 1998.
- Bassiouny, H. S., S. White, S. Glagov, E. Choi, D. P. Giddens, and C. K. Zarins. Anastomotic intimal hyperplasia: Mechanical injury or flow induced. *J. Vasc. Surg.* 15:708–717, 1992.
- Botnar, R., G. Rappitsch, M. B. Scheidegger, D. Leipsch, K. Perktold, and P. Boesiger. Hemodynamics in the carotid artery bifurcation: A comparison between numerical simulations and *in vitro* MRI measurements. *J. Biomech.* 33:137–144, 2000.
- Buonocore, M. H., and H. Bogren. Factors influencing the accuracy and precision of velocity-encoded phase imaging. *Magn. Reson. Med.* 26:141–54, 1992.

- <sup>5</sup>Buonocore, M. H., L. Gao, and H. G. Bogren. Experimental study of the effects of fractional gating on flow measurements. *J. Magn. Reson. Imaging* 2:142, 1992.
- <sup>6</sup>Ethier, C., D. A. Steinman, X. Zhang, S. R. Karpik, and M. Ojha. Flow waveform effects on end-to-side anastomotic flow patterns. *J. Biomech.* 31:609–617, 1998.
- <sup>7</sup>Favier V., and C. A. Taylor. Modeling blood flow in a porcine aorta bypass graft: Toward physiological conditions. Center for Turbulence Research Annual Research Briefs, 2001, pp. 219–230.
- <sup>8</sup>Fei, D., J. Thomas, and S. Rittgers. The effect of angle and flow rate upon hemodynamics in distal vascular graft anastomoses: A numerical study. *J. Biomech. Eng.* 116:331–336, 1994.
- <sup>9</sup>Fredrickson, J. O., and N. J. Pelc. Time-resolved MR imaging by automatic data segmentation. *J. Magn. Reson. Imaging* 4:189–196, 1994.
- <sup>10</sup>Hofer, M., K. Rappitsch, W. Perktold, W. Trubel, and H. Schima. Numerical study of wall mechanics and fluid dynamics in end-to-side anastomoses and correlation to intimal hyperplasia. *J. Biomech.* 29:1297–1308, 1996.
- <sup>11</sup>Kim, Y. H., K. B. Chandran, T. J. Bower, and J. D. Corson. Flow dynamics across end-to-end vascular bypass graft anastomoses. *Ann. Biomed. Eng.* 21:311–320, 1993.
- <sup>12</sup>Lee, D., and J. J. Chiu. Intimal thickening under shear in a carotid bifurcation—A numerical study. *J. Biomech.* 29:1–11, 1996.
- <sup>13</sup>Lei, M., C. Kleinstreuer, and G. A. Truskey. Numerical investigation and prediction of atherogenic sites in branching arteries. *J. Biomech. Eng.* 117:350–357, 1995.
- <sup>14</sup>Lei, M., C. Kleinstreuer, and J. Archie, Jr. Geometric design improvements for femoral graft–artery junctions mitigating restenosis. *J. Biomech.* 29:1605–1614, 1996.
- <sup>15</sup>Lei, M., J. P. Archie, and C. Kleinstreuer. Computational design of a bypass graft that minimizes wall shear stress gradients in the region of the distal anastomosis. *J. Vasc. Surg.* 25:637–646, 1997.
- <sup>16</sup>Lei, M., D. Giddens, S. Jones, F. Loth, and H. Bassiouny. Pulsatile flow in an end-to-side vascular graft model: Comparison of computations with experimental data. *J. Biomech. Eng.* 123:80–87, 2001.
- <sup>17</sup>Long, Q., X. Y. Xu, B. Ariff, S. A. Thom, A. D. Hughes, and A. V. Stanton. Reconstruction of blood flow patterns in a human carotid bifurcation: A combined CFD and MRI study. *J. Magn. Reson. Imaging* 11:299–311, 2000.
- <sup>18</sup>Long, Q. X. Y. Xu, M. Bourne, and T. M. Griffith. Numerical study of blood flow in an anatomically realistic aorto–iliac bifurcation generated from MRI data. *Magn. Reson. Med.* 43:565–576, 2000.
- <sup>19</sup>Moser, K. W., E. C. Kutter, J. G. Georgiadis, R. O. Buckius, H. D. Morris, and J. R. Torczynski. Velocity measurements of flow through a step stenosis using magnetic resonance imaging. *Exp. Fluids* 29:438–447, 2000.
- <sup>20</sup>Naylor, G. L., D. N. Firmin, and D. B. Longmore. Blood flow imaging by cine magnetic resonance. *J. Comput. Assist. Tomogr.* 10:715–22, 1986.
- <sup>21</sup>Papaharilaou, Y., D. Doorly, S. Sherwin, J. Peiro, J. Anderson, B. Sanghera, N. Watkins, and C. Caro. Combined MRI and computational fluid dynamics detailed investigation of flow in a realistic coronary artery bypass graft model. International Society for Magnetic Resonance in Medicine. Glasgow, Scotland: 2001, p. 379.
- <sup>22</sup>Pelc, N. J., R. J. Herfkens, A. Shimakawa, and D. R. Enzmann. Phase contrast cine magnetic resonance imaging. *Magn. Reson. Q.* 7:229–254, 1991.
- <sup>23</sup>Pelc, N. J., F. G. Sommer, K. C. P. Li, T. J. Brosnan, R. J. Herfkens, and D. R. Enzmann. Quantitative magnetic resonance flow imaging. *Magn. Reson. Q.* 10:125–147, 1994.
- <sup>24</sup>Pelc, N. J. Flow quantification and analysis methods. *Magn. Reson. Imaging Clin. N. Am.* 3:413–424, 1995.
- <sup>25</sup>Perktold, K., and G. Rappitsch. Computer simulation of local blood flow and vessel mechanics in a compliant carotid artery bifurcation model. *J. Biomech.* 28:845–856, 1995.
- <sup>26</sup>Shephard, M. S. Meshing environment for geometry-based analysis. *Int. J. Numer. Methods Eng.* 47:169–190, 2000.
- <sup>27</sup>Steinman, D. A., and C. R. Ethier. The effect of wall distensibility on flow in a two-dimensional end-to-side anastomosis. *J. Biomech. Eng.* 116:294–301, 1994.
- <sup>28</sup>Steinman, D. A., R. Frayne, X. D. Zhang, B. K. Rutt, and C. R. Ethier. MR measurement and numerical simulation of steady flow in an end-to-end anastomosis model. *J. Biomech.* 29:537–542, 1996.
- <sup>29</sup>Steinman, D. A., C. R. Ethier, X. Zhang, and S. Karpik. Effects of local geometry on anastomotic flow patterns. *Adv. Bioeng.* 28:433–434, 1994.
- <sup>30</sup>Taylor, C. A., T. J. R. Hughes, and C. K. Zarins. Finite element modeling of blood flow in arteries. *Comput. Methods Appl. Mech. Eng.* 158:155–196, 1998.
- <sup>31</sup>Taylor, C. A., T. J. R. Hughes, and C. K. Zarins. Finite element modeling of three-dimensional pulsatile flow in the abdominal aorta: Relevance to atherosclerosis. *Ann. Biomed. Eng.* 26:1–14, 1998.
- <sup>32</sup>Taylor, C. A., M. T. Draney, J. P. Ku, D. Parker, B. N. Steele, K. Wang, and C. K. Zarins. Predictive medicine: Computational techniques in therapeutic decision making. *Comput. Aided Surg.* 4:231–247, 1999.
- <sup>33</sup>Taylor, C. A., T. J. Hughes, and C. K. Zarins. Effect of exercise on hemodynamic conditions in the abdominal aorta. *J. Vasc. Surg.* 29:1077–1089, 1999.
- <sup>34</sup>Thomsen, C., M. Corsten, L. Sondergaard, O. Henriskon, and F. Stahlberg. A segmental *k*-space velocity mapping protocol for quantification of renal artery blood flow during breath holding. *J. Magn. Reson. Imaging* 5:393–401, 1995.
- <sup>35</sup>Wang, K. C., R. W. Dutton, and C. A. Taylor. Level sets for vascular model construction in computational hemodynamics. *IEEE Eng. Med. Biol. Mag.* 18:33–39, 1999.
- <sup>36</sup>Wang, K. C. Level set methods for computational prototyping with application to hemodynamic modeling. Electrical Engineering, Stanford, CA: Stanford University, 2001.
- <sup>37</sup>Wedding, K. L., M. T. Draney, R. J. Herfkens, C. K. Zarins, C. A. Taylor, and N. J. Pelc. Measurements of *in vivo* vessel wall motion and strain with cine phase contrast MRI. In: Proceedings of the International Society for Magnetic Resonance in Medicine 8th Scientific Meeting and Exhibition, Denver, CO, 2000, Abstract No. 1652.
- <sup>38</sup>Zarins, C. K., D. P. Giddens, B. K. Bharadvaj, V. S. Sottiurai, R. F. Mabon, and S. Glagov. Carotid bifurcation atherosclerosis: Quantitative correlation of plaque localization with flow velocity profiles and wall shear stress. *Circ. Res.* 53:502–514, 1983.